

Early Bearing Fault Detection Using EEMD and Three-Sigma Rule Denoising Method

Yasser DAMINE*, Nouredine BESSOUS**, Ahmed Chaouki MEGHERBI***, Salim SBAA****

*University of Mohamed Khider Biskra, Laboratory of LI3CUB, Algeria, E-mail: yasser.damine@univ-biskra.dz

**University of El-Oued, Laboratory of LGEERE, Algeria, E-mail: bessous-nouredine@univ-eloued.dz

***University of Mohamed Khider Biskra, Laboratory of LI3CUB, Algeria, E-mail: ac.megherbi@univ-biskra.dz

****University of Mohamed Khider Biskra, Laboratory of VSC, Algeria, E-mail: s.sbaa@univ-biskra.dz

<https://doi.org/10.5755/j02.mech.32770>

1. Introduction

It's known that 90% of the energy consumed by the industry is derived from induction machines. Several faults are often responsible for unexpected failures. Study results indicate that bearing faults are responsible for a high percentage of failures in induction machines. This makes it highly recommended that small and medium voltage induction machines are continuously monitored for bearing faults [1, 2]. It is possible to gain rich information about the machine's health from vibration signals [3].

Many researchers employ appropriate techniques to extract fault information from the non-stationary and nonlinear vibration signals of rolling bearings. The empirical mode decomposition (EMD) is a time-frequency analysis technique developed by Huang et al. [4]. The EMD does not rely on the basis function like the short-time Fourier transform or wavelet transform. It decomposes signals into oscillatory components known as intrinsic mode functions (IMFs). The EMD technique has been widely used to analyze bearing fault vibration signals. However, a significant problem with EMD is mode mixing. To solve this problem, Wu and Huang. [5] proposed Ensemble Empirical Mode Decomposition (EEMD), an improved version of EMD. Compared to the EMD, it has been shown that IMFs produced by the EEMD can better highlight the characteristics of the signal [6].

Background noise is a significant factor affecting the performance of EEMD, combining EEMD with other techniques is necessary for improving bearing fault diagnosis [7-9]. By using EEMD and Wavelet Packet Transforms, Xie et al. [7] proposed a method for de-noising Bearing Vibration Signals. Based on EEMD and envelope spectrum analysis, Xu et al. [8] developed a method for diagnosing bearing faults. Li et al. [9] presented a bearing fault diagnosis based on EEMD and index of envelope spectrum sparse ratio.

Considering the above, this paper proposes a fault diagnosis method combining EEMD and a denoising approach based on the three-sigma rule to purify the raw signal and to extract the defect information, respectively. Firstly, the bearing signal is decomposed by EEMD into IMF components, then the kurtosis of each component is calculated. After that, the components that have significant values are selected for reconstruction. To enhance fault detection, the reconstructed signal is de-noised using the

three-sigma de-noising method. Finally, the processed signal is analyzed by envelope spectrum to determine the fault characteristic frequency.

The other parts of this paper are as follows. Section 2 is divided into three parts which give the representations of the theoretical backgrounds of EEMD, Kurtosis, and the Three-sigma de-noising method, respectively. Section 3 describes the proposed bearing fault diagnosis method. Section 4 presents the results of applying the proposed method to experimental data. The conclusion of this paper is given in section 5.

2. Basic principle

2.1. EEMD algorithm

The EEMD algorithm solves the problem of EMD by eliminating the mode mixing phenomenon. In addition, it provides more accurate fault information for rolling element bearings compared to EMD. The EEMD algorithm proceeds as follows [10].

Step 1. Add the white Gaussian noise to the original signal with a mean of 0 and the standard deviation of 1 and get:

$$X_i = X + \beta w_i, \quad (1)$$

where: w_i is the i^{th} added white noise for $i=1,2, \dots, I$. where I indicate the number of realizations, and β means the amplitude of the i^{th} added white noise.

Step 2. To obtain the IMF_{ij} , it's necessary to decompose each X_i by EMD, where ($j=1, \dots, N$), N indicates the number of IMFs, and r_i is the residue of the i^{th} realization.

$$X_i = \sum_{j=1}^N IMF_{ij} + r_i. \quad (2)$$

Step 3: Based to determine the ensemble means $I IMF_j$ of the I trials as shown in the following formula:

$$IMF_j = \sum_{i=1}^I IMF_{ij}, \quad (3)$$

where: IMF_j is the i^{th} IMF ($IMF_1, IMF_2, \dots, IMF_N$) decomposed by EEMD.

2.2. Kurtosis

Kurtosis is an indicator that measures the peak degree of a signal waveform. As the proportion of impact components increases, the kurtosis value also increases. In the absence of rolling defects, the kurtosis approaches a Gaussian distribution; however, if impulses occur, the kurtosis increases significantly. Kurtosis can be expressed as follows:

$$K = \frac{1}{N} \sum_{i=1}^N \frac{(x_i - \mu)^4}{\sigma^2}, \quad (4)$$

where: μ denotes the signal's average; σ denotes its standard deviation; N is the number of samples; x_i denotes the vibration's amplitude over time [11].

2.3. Three-sigma rule denoising method

According to the three-sigma rule, 99.73% of data that follows a normal distribution lies within three standard deviations from a mean [12].

$$P\{\mu - 3\sigma < X < \mu + 3\sigma\} \approx 99.73\%. \quad (5)$$

The mean and standard deviation are represented by μ and σ , respectively. The normal distribution appears with:

$$E(X) = \mu = 0, \quad (6)$$

$$D(X) = E(X^2) - [E(X)]^2 = E(X^2) = \sigma^2, \quad (7)$$

where: $E(X)$ and $D(X)$ are representations of the expectation and variance of X , respectively.

As a result of Eq. (7), X has the following root mean square (RMS) value:

$$\begin{aligned} X_{rms} &= \sqrt{\frac{1}{N} \sum_{i=1}^n [x_i - E(X)]^2} = \sqrt{\frac{1}{N} \sum_{i=1}^n x_i^2} = \\ &= \sqrt{E(X^2)} = \sigma, \end{aligned} \quad (8)$$

where: x_i is the time-domain sampling data of X and n indicates the sampling number.

Using Eq. (6) and Eq. (8), Eq. (9) can be written as:

$$\begin{aligned} P\{-3\sigma < X < +3\sigma\} &= \\ = P\{-3X_{rms} < X < +3X_{rms}\} &\approx 99.73\%. \end{aligned} \quad (9)$$

Based on the assumption that a fault-free rolling bearing follows a normal distribution [13], Eq. (9) shows that almost all the noise in the bearing vibration signal X is distributed within $\pm X_{rms}$. Due to this, it is necessary to remove the components within $\pm X_{rms}$. The denoising process consists of the following steps [14]:

1. Zero-mean normalization is applied to X :

$$Y(t) = \frac{X - \mu}{\sigma}, \quad (10)$$

where: $Y(t)$ is the normalized signal.

2. Determine the root mean square value Y_{rms} of $Y(t)$.

3. Replace the sampling data y_i of $Y(t)$ falling between $\pm 3Y_{rms}$ with zero while leaving y_i outside of $\pm 3Y_{rms}$ unchanged. The process may be presented by:

$$\begin{cases} Z = 0 & \text{if } |y_i| \leq 3Y_{rms} \\ Z = y_i(t) & \text{otherwise} \end{cases}, \quad (11)$$

where: $X(t)$ is represented by $Z(t)$ after removing the unnecessary components.

3. The proposed fault diagnosis of rolling bearing based on EEMD and the three-sigma rule denoising

The bearing signal is decomposed into IMF components by EEMD, and the kurtosis for each component is calculated. For reconstruction, the components with significant values are selected. Then, the three-sigma rule denoising is applied to the reconstructed signal to enhance fault detection. After the signal has been processed, it is analyzed using the envelope spectrum. Fig. 1 illustrates the flow chart of the bearing fault detection method. The detailed description of the flow chart is as follows:

Step 1. Decompose the fault vibration signal with defect into IMFs by EEMD.

Step 2. Calculate the kurtosis of each IMF component.

Step 3. Select the appropriate IMFs based on the high values of kurtosis

Step 4. Reconstruct the signal by the selected IMFs.

Step 5. Perform the three-sigma denoising method on the reconstructed signal. It consists of a few steps:

1) Normalize the reconstructed signal using Zero mean normalization.

2) Calculate the root mean square value Y_{rms} of the normalized signal.

3) Replace the sampling data of the normalized signal with zero if it falls between $\pm 3Y_{rms}$ while keeping the sampling data outside of $\pm 3Y_{rms}$ unchanged.

Step6. The processed signal is analyzed by envelope spectrum.

4. Experimental validation

Data from Case Western Reserve University [15] was used to validate the proposed method's effectiveness in detecting bearing faults. Fig. 2 shows a dynamometer consisting of a motor with a power output of two horsepower (left), a torque sensor/encoder in the center, a dynamometer in the right, and control electronics. Due to electro-discharge machining, we have three types of faults: outer race fault, inner race fault, and ball fault. Rotation speed ranged from 1730 to 1797 RPM. In this study, we used the time signals recorded for the inner race and outer race fault of the drive end bearing. 12000 samples were collected per second for this vibration signal. This experimental test was performed using a deep groove ball bearing 6205-2RS JEM SKF. The bearing parameters are listed in Table 1.

Table 1

Parameters of the bearing 6205-2rs jem skf

Inside diameter	25 mm
Outside diameter	52 mm
Intermediate diameter	39 mm
Ball diameter	8
Number of rollers	9
Contact angle	0 rad

When the bearing defect occurs in its early stages, it is localized: it consists of a crack or spall. The inner and outer rings of rolling elements generate shock impulses every time they hit a local fault. Repeated shock pulses cause vibrations at the frequency corresponding to the faulty component. BPF_I (Ball Passing Frequency Inner

Race) and BPF_O (Ball Passing Frequency Outer Race) are both fault characteristic frequencies, which refer to the inner race and outer race, respectively. The following are their mathematical equations [16]:

$$F_{BPF_I} = \frac{F_r}{2} N_b \left(1 + \frac{D_b \cos \beta}{D_c} \right), \quad (12)$$

$$F_{BPF_O} = \frac{F_r}{2} N_b \left(1 - \frac{D_b \cos \beta}{D_c} \right), \quad (13)$$

where: F_r is the rotor shaft frequency; N_b is the number of rolling elements; D_c is the pitch diameter; D_b is the ball diameter, and β is the ball contact angle.

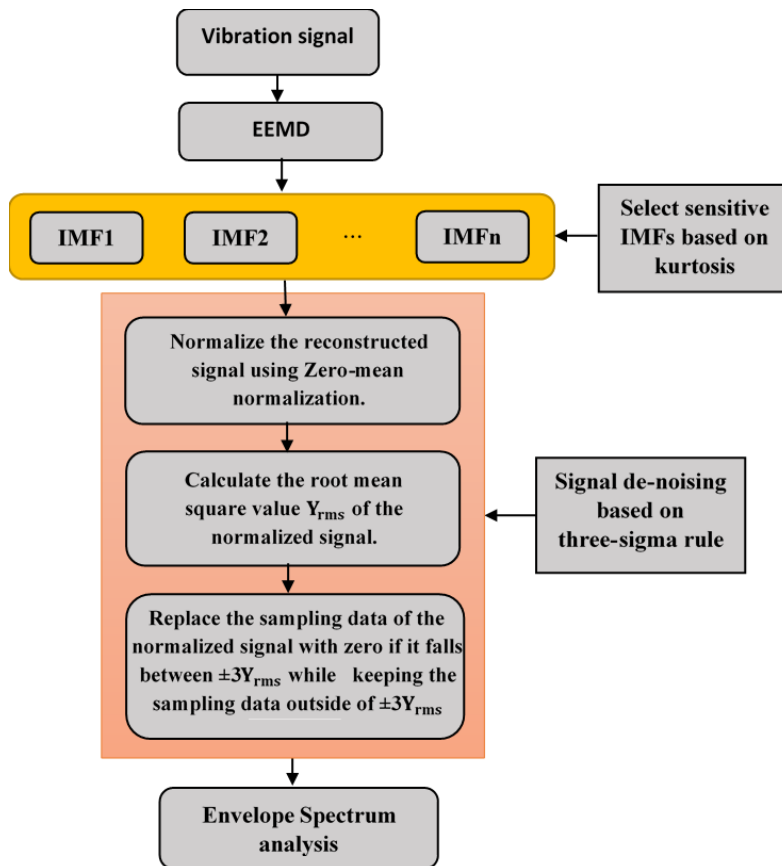


Fig. 1 Flowchart of the bearing fault diagnosis method

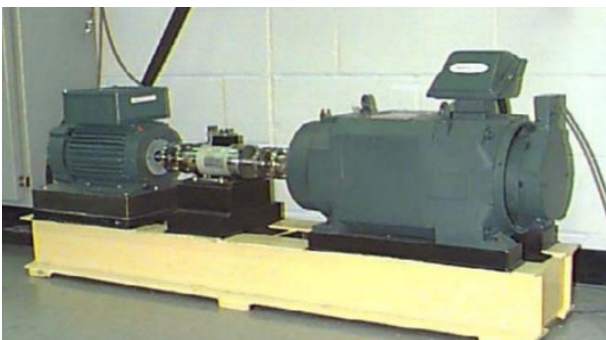


Fig. 2 Experimental test rig from CWRW [15]

4.1. The inner race fault analysis

Here, the vibration signal emanating from the inner race fault is analyzed using the method presented in the

paper (Fig. 1). There is a shaft speed of 1750 rpm, a load of 2 hp, and a fault size of 0.007 inches. A fault characteristic frequency of 157.9 Hz can be calculated for the inner race based on the parameters in Table 1 and Eq. (12). Analyzing 24000 data points, the measured original bearing signal with the inner race fault signal is plotted in Fig. 3, a. There is a noise effect that prevents the periodic impulses from being extracted. From the envelope spectrum in Fig. 3b, the fault characteristic f_i and the first harmonic can be determined. However, the other harmonics are obscured by noise interference. Thus, pre-processing is required to improve fault detection.

4.1.1. Application of the proposed method

To demonstrate the effectiveness of the proposed method, EEMD decomposition is applied to the measured

signal and the first five IMFs are plotted in Fig. 4. The kurtosis values of these IMFs are shown in Table 2. Clearly, IMF 1, IMF 2, and IMF 3 have the highest values among all the decomposition results, so these IMFs are selected for signal reconstruction. To reduce noise in the reconstructed signal, the three-sigma rule de-noising technique (described in section 3) is applied. In the first step, the reconstructed signal is normalized by zero-mean normalization. Following this, the root means square value of the normalized signal is calculated, and the components within $\pm 3Y_{rms}$ are removed. The result of de-noising is shown in Fig. 5a. It is observed that the noise level is reduced effectively, as well as periodic fault impulses are emphasized. From the envelope spectrum in Fig. 5b and compared with the envelope spectrum of the original signal in Fig. 3b, it is evident that we can extract the inner race fault characteristic frequency f_i and more fault information ($2f_i, 3f_i, 4f_i, 5f_i, 6f_i$ and $7f_i$). The results demonstrate that the method presented in this paper can accurately diagnose the bearing with an inner race fault.

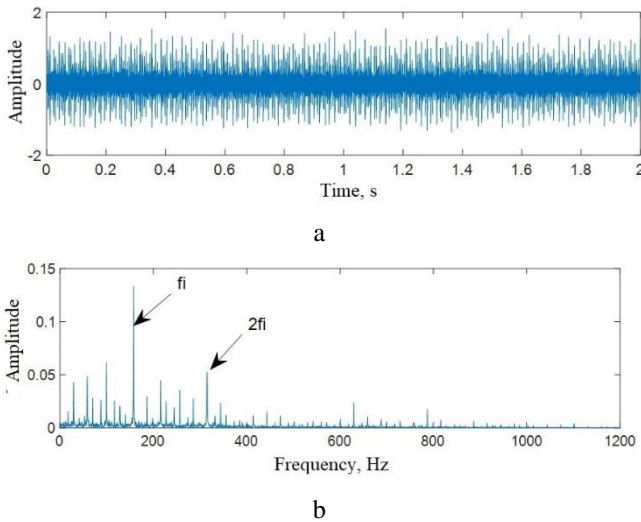


Fig. 3 Original vibration signal with inner race defect: a) time domain waveform; b) envelope spectrum

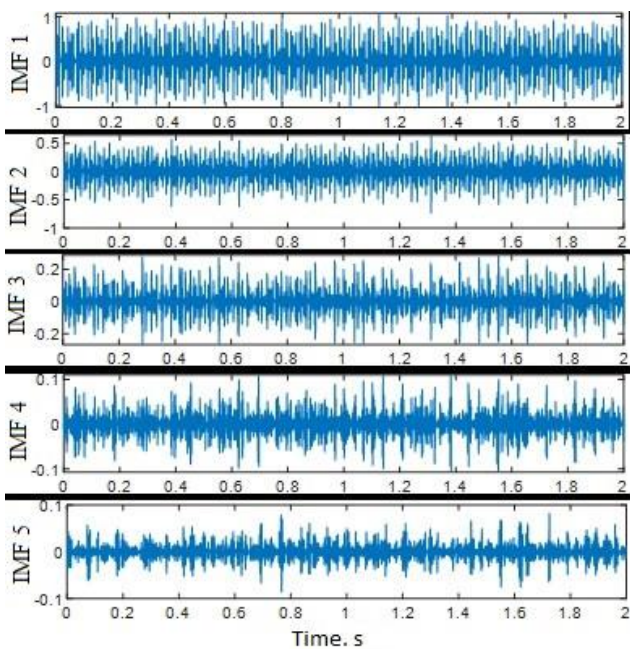


Fig. 4 Decomposed result of the original signal by EEMD

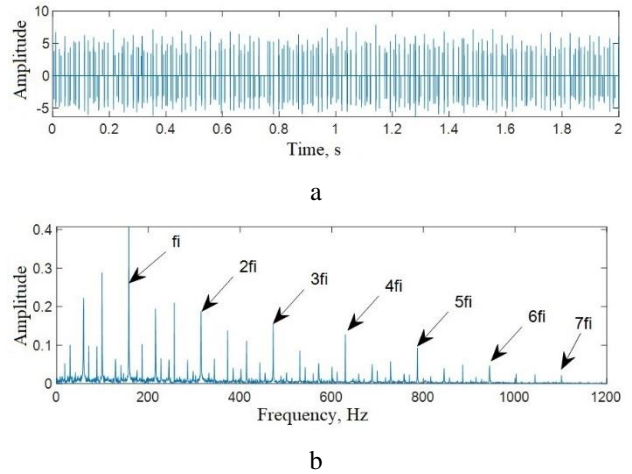


Fig. 5 a) The resulting signal obtained by the proposed method; b) envelope spectrum

Table 2

Kurtosis values of each IMF

IMF	Kurtosis
IMF1	8,51
IMF2	5,84
IMF3	6,42
IMF4	5,30
IMF5	4,97

4.1.2. Comparison with EEMD

Fig. 6a shows the reconstructed signal with effective IMFs, while Fig. 6b shows its envelope spectrum. By comparing Fig. 5a with Fig. 6a, it is clear that the method described in this paper suppresses noise and emphasizes fault impulses more effectively than the EEMD method. Comparing the envelope spectrums in Fig. 5b and Fig. 6b, this method can also provide more fault information ($2f_i, 3f_i, 4f_i, 5f_i, 6f_i$ and $7f_i$) than the EEMD. The comparison results reveal that the proposed method is superior and more effective for improving fault detection.

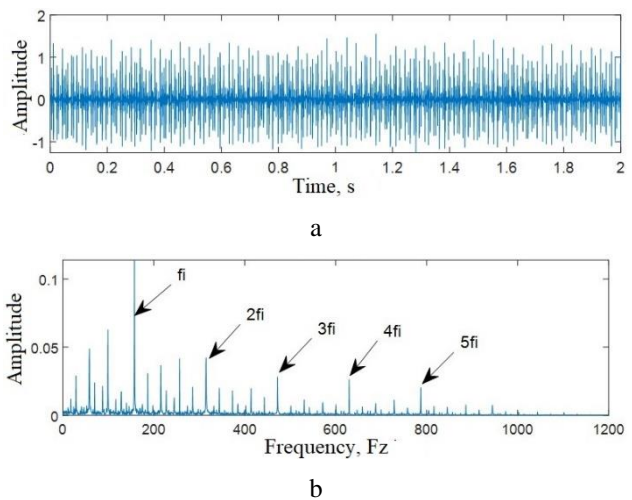


Fig. 6 a) The resulting signal obtained by EEMD; b) envelope spectrum

4.2. The outer race fault analysis

In this case, the vibration signal emanating from the outer race fault is analyzed. There is a shaft speed of 1797 rpm, a load of 0 hp, and a fault size of 0.021 inches.

A fault characteristic frequency of 107.01 Hz can be calculated for the outer race based on the parameters in Table 1 and Eq. (13). Analyzing 24000 data points, the original bearing signal with the outer race fault signal is plotted in Fig. 7, a and its envelope spectrum is shown in Fig. 3, b. It can be seen that the fault characteristic frequency of the outer race and the first harmonic can be determined. However, noise interference obstructs the other harmonics. Therefore, pre-processing is required to improve fault detection.

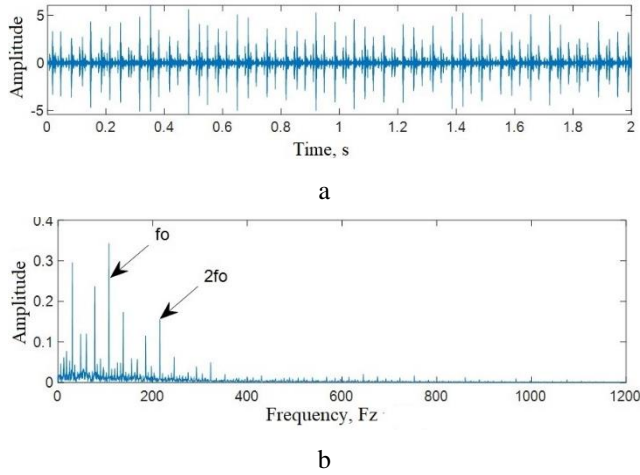


Fig. 7 Original vibration signal with outer race defect: a) time domain waveform; b) envelope spectrum

4.2.1. Application of the proposed method

To illustrate the advantages of the proposed approach for improving fault detection, EEMD decomposition is applied to the measured signal and the first five IMFs are plotted in Fig. 8.

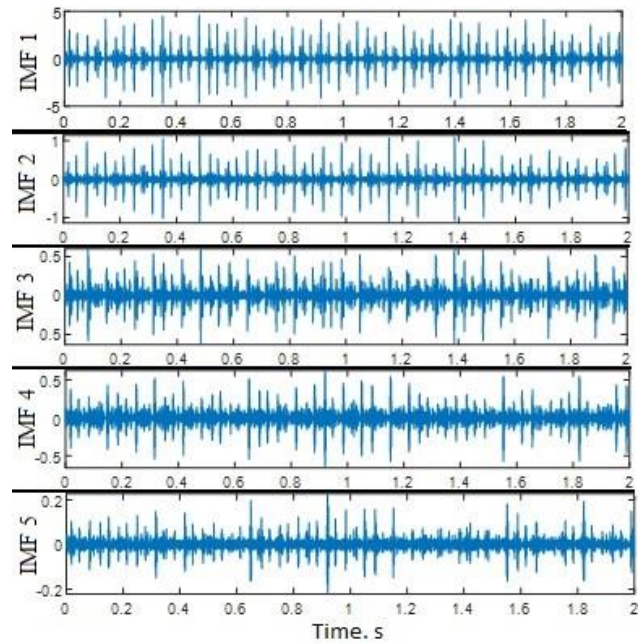


Fig. 8 Decomposed result of the original signal by EEMD

Table 3 shows the kurtosis values of these IMFs. It is evident that IMF1 and IMF2 have significant values, so these IMFs are selected for signal reconstruction. To reduce noise in the reconstructed signal, the three-sigma

rule de-noising technique is applied. First, the reconstructed signal is normalized by Zero-mean normalization. In the next step, the root means square value Y_{rms} of the normalized signal is calculated and the components within $\pm 3Y_{rms}$ are removed. Fig. 9, a show the signal after denoising, it can be seen that the noise level is effectively reduced, and the periodic fault impulses are emphasized. From the envelope spectrum in Fig. 9, b and compared with the envelope spectrum of the original signal in Fig. 7, b, it is clear that we can extract the outer race fault characteristic frequency f_o and more fault information ($2f_o, 3f_o, 4f_o, 5f_o, 6f_o$ and $7f_o$). Consequently, the results demonstrate that the bearing with the outer race fault can be accurately diagnosed by the proposed technique.

Table 3

Kurtosis values of each IMF

IMF	Kurtosis
IMF1	17,70
IMF2	25,19
IMF3	10,60
IMF4	8,84
IMF5	10,06

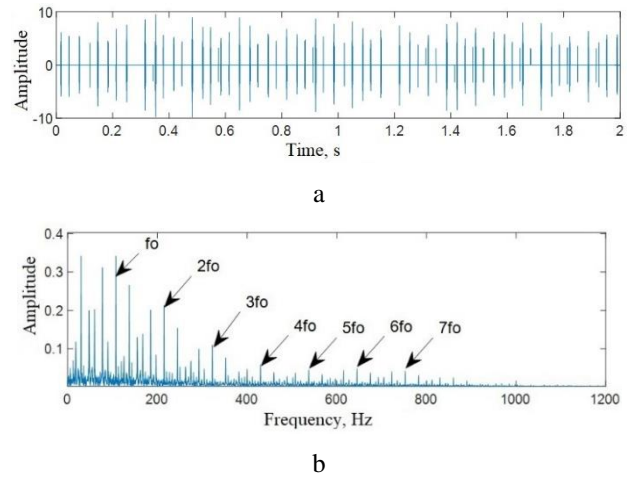


Fig. 9 a) The resulting signal obtained by the proposed method; b) envelope spectrum

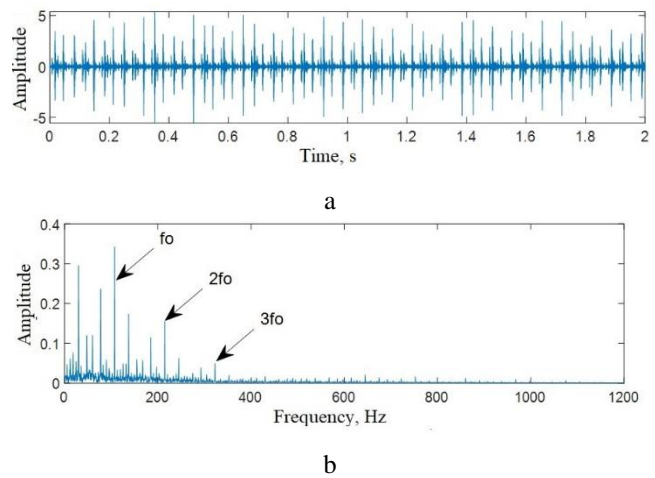


Fig. 10 a) The resulting signal obtained by EEMD; b) envelope spectrum

4.2.2. Comparison with EEMD

The reconstructed signal with effective IMFs is

shown in Fig. 10, a and its envelope spectrum is shown in Fig. 10, b. Comparing Fig. 9, a with Fig. 10, a, it is clear that the method presented in this paper eliminates the noise and emphasizes the fault impulses more effectively than the EEMD. Comparing the envelope spectrums in Fig. 9, b and Fig. 10, b, this method can also extract more fault information ($2f_o$, $3f_o$, $4f_o$, $5f_o$, $6f_o$ and $7f_o$). The comparison results reveal that the method proposed here is superior and more effective for improving fault detection.

5. Conclusion

In this paper, a rolling bearing fault diagnosis technique is proposed by combining EEMD with the three-sigma rule de-noising technique. From the analysis of the experimental bearing fault vibration signal, we found that:

1. Noise can be effectively reduced and the periodic impulses can be successfully improved using the proposed method.

2. The proposed method can effectively extract rich fault information from the envelope spectrum

3. In comparison with the EEMD, the proposed method is more effective for improving fault detection.

References

1. **Kompella, K.; Rao, M.; Rao, R.** 2018. Bearing fault detection in a 3-phase induction motor using stator current frequency spectral subtraction with various wavelet decomposition techniques, *Ain Shams Engineering Journal* 9(4): 2427-2439. <https://doi.org/10.1016/j.asej.2017.06.002>.
2. **Kumar, P.; Kumaraswamidhas, L.; Laha, S.** 2019. Selecting effective intrinsic mode functions of empirical mode decomposition and variational mode decomposition using dynamic time warping algorithm for rolling element bearing fault diagnosis, *Transactions of the Institute of Measurement and Control* 41(7): 1923-1932. <https://doi.org/10.1177/0142331218790788>.
3. **Zhang, W.; Peng, G.; Li, C.** 2017. Bearings fault diagnosis based on convolutional neural networks with 2-D representation of vibration signals as input, In *MATEC web of conferences*. <https://doi.org/10.1051/mateconf/20179513001>.
4. **Huang, N.; Shen, Z.; Long, S.; Wu, M.; Shih, H.; Zheng, Q.; Liu, H.** 1998. The empirical mode decomposition and the Hilbert spectrum for nonlinear and non-stationary time series analysis, *Proceedings of the Royal Society of London. Series A: mathematical, physical and engineering sciences* 454(1971): 903-995. <https://doi.org/10.1098/rspa.1998.0193>.
5. **Wu, Z.; Huang, N.** 2009. Ensemble empirical mode decomposition: a noise-assisted data analysis method, *Advances in adaptive data analysis* 1(01): 1-41. <https://doi.org/10.1142/S1793536909000047>.
6. **Fang, K.; Zhang, H.; Qi, H.; Dai, Y.** 2018. Comparison of EMD and EEMD in rolling bearing fault signal analysis, *IEEE International Instrumentation and Measurement Technology Conference*. <https://doi.org/10.1109/I2MTC.2018.8409666>.
7. **Xie, S.; Zhang, W.; Lu, Y.; Shao, X.; Chen, D.; Lu, Q.** 2020. Denoising method for bearing vibration signal based on EEMD and wavelet packet transform, 10th Institute of Electrical and Electronics Engineers International Conference on Cyber Technology in Automation, Control, and Intelligent Systems, p. 277-282. <https://doi.org/10.1109/CYBER50695.2020.9279184>.
8. **Xu, Y.; Wang, H.; Zhou, Z.; Chen, W.** 2021. Diagnosis of weak fault of rolling bearing based on EEMD and envelope spectrum analysis, 3rd International Symposium on Robotics & Intelligent Manufacturing Technology, p. 419-422. <https://doi.org/10.1109/ISRIMT53730.2021.9596987>.
9. **Li, Z.; Zhang, M.; Li, L.; Chen, R.; Zhang, Y.; Cui, Y.** 2021. Rolling element bearing fault diagnosis based on EEMD and index of envelope spectrum sparse ratio, *International Conference on Intelligent Transportation, Big Data & Smart City*, p. 338-341. <https://doi.org/10.1109/ICITBS53129.2021.00090>.
10. **Lei, Y.; Lin, J.; He, Z.; Zuo, M.** 2013. A review on empirical mode decomposition in fault diagnosis of rotating machinery, *Mechanical systems and signal processing* 35(1-2): 108-126. <https://doi.org/10.1016/j.ymssp.2012.09.015>.
11. **Wang, Y.; Xiang, J.; Markert, R.; Liang, M.** 2016. Spectral kurtosis for fault detection, diagnosis and prognostics of rotating machines: A review with applications, *Mechanical Systems and Signal Processing* 66: 679-698. <https://doi.org/10.1016/j.ymssp.2015.04.039>.
12. **Zhao, H.; Min, F.; Zhu, W.** 2013. Test-cost-sensitive attribute reduction of data with normal distribution measurement errors, *Mathematical Problems in Engineering*. <https://doi.org/10.1155/2013/946070>.
13. **Qin, B.; Luo, Q.; Zhang, J., Li, Z., & Qin, Y.** 2021. Fault frequency identification of rolling bearing using reinforced ensemble local mean decomposition, *Journal of Control Science and Engineering*. <https://doi.org/10.1155/2021/2744193>.
14. **Wang, H.; Deng, S.; Yang, J.; Liao, H.** 2019. A fault diagnosis method for rolling element bearing (REB) based on reducing REB foundation vibration and noise-assisted vibration signal analysis, *Proceedings of the Institution of Mechanical Engineers, Part C: Journal of Mechanical Engineering Science* 233(7): 2574-2587. <https://doi.org/10.1177/0954406218791209>.
15. **Loparo, K. A.** 2021. Case School of Engineering: Case Western Reserve University. Case School of Engineering. <https://engineering.case.edu/bearingdatacenter/download-data-file>.
16. **Saruhan, H.; Saridemir, S.; Qicek, A.; Uygur, I.** 2014. Vibration analysis of rolling element bearings defects, *Journal of applied research and technology* 12(3): 384-395. [https://doi.org/10.1016/S1665-6423\(14\)71620-7](https://doi.org/10.1016/S1665-6423(14)71620-7).

Y. Damine, N. Bessous, A.C. Megherbi, S. Sbaa

EARLY BEARING FAULT DETECTION USING EEMD AND THREE-SIGMA RULE DENOISING METHOD

S u m m a r y

Rotating electrical machines have several physical phenomena. Vibration is one of the important phenomena in the operation of rotating electrical machines. In addition, the vibration signal is considered an important source to have good information on the state of rotating electrical machinery. But this signal is rich in noise, especially under the presence of the bearing fault. This paper proposes a bearing fault diagnosis method based on EEMD and a denoising method based on three-sigma rule. In the first step, the EEMD decomposed the vibration signal into several components called Intrinsic Mode Functions

(IMFs). After the calculation of the kurtosis of each IMF component, the signal is reconstructed by choosing components with higher values. To enhance periodic impulses, the three-sigma rule de-noising is applied to the reconstructed signal. As a final step, the envelope spectrum is used to determine the fault characteristic frequency. As a result of testing the bearing with inner race fault and the bearing with outer race, it was verified that the proposed approach suppressed noise effectively and extracted rich fault information from the vibration signals of bearings compared to the EEMD.

Keywords: Bearing Fault diagnosis, signal denoising, ensemble empirical mode decomposition, early fault detection.

Received November 14, 2022

Accepted August 2, 2023



This article is an Open Access article distributed under the terms and conditions of the Creative Commons Attribution 4.0 (CC BY 4.0) License (<http://creativecommons.org/licenses/by/4.0/>).